cerebral blood volume (CBV) to the kinetic $^{15}O_2$ data obtained from a single PET scan after the bolus administration of $^{15}O_2$. To minimize errors which result from neglecting RW, only the initial 3 mins of data after the bolus inhalation of $^{15}O_2$ were used when calculating the parameters. This approach has been applied to evaluate the magnitude of increase in $CMRO_2$ relative to that in CBF during cognitive stimulation tasks (Fujita *et al*, 1999; Vafaee and Gjedde, 2000; Okazawa *et al*, 2001*a*,*b*; Yamauchi *et al*, 2003; Mintun *et al*, 2002), but one of the drawbacks to this technique is the lack of accurate statistics, which is due to the use of a short scan duration.

Iida *et al* (1993) have developed a mathematical formula to predict the production of RW based on a physiologic model, which allows prolongation of the PET acquisition period with an additional statistical accuracy. The formula assumes a fixed rate constant for production of RW from $^{15}O_2$ in the body. This is based on the fact that the observed rate constant did not vary among clinical subjects, and thus causes nonsignificant errors in $CMRO_2$. However, the study is limited only to human subjects studied at rest, and results have not been verified using other species such as rat and mouse (Magata *et al*, 2003; Temma *et al*, 2006; Yee *et al*, 2006). Also, the findings have not been evaluated on humans who are under physiologic stress, though under such conditions the whole-body oxygen consumption is expected to change. Moreover, it is important to extend the approach to physiologically stressed conditions as recent progress for assessing $CMRO_2$ and CBF simultaneously from a short period dynamic scan by using a dual tracer autoradiography (DARG) (Kudomi *et al*, 2005). The DARG has enabled the $^{15}O_2$ PET to assess $CMRO_2$ and CBF simultaneously at various physiologically activated conditions.

The aim of this study is to verify the method used to estimate the arterial RW during the $^{15}O_2$ inhalation for simultaneous determination of $CMRO_2$ and CBF from the rapid procedures of $^{15}O_2$ PET. The feasibility of a simplified procedure is also being investigated. Applicability of this approach was tested for a wide range of species under various physiologic conditions. Experiments were designed to apply for different species as well as different physiologic conditions. A simulation study was also performed to evaluate the level of error sensitivity associated with this approach.

Materials and methods

Theory

Variables used in the recirculating water model are summarized in Table 1. The mathematical model that formulates the time-dependent RW in arterial blood consists of three rate constants: (1) the production rate of RW or k (per min), proportional to oxidative metabolism in the total body system ($BMRO_2$), (2) the forward diffusion rate (k_w, per min) of the metabolized ^{15}O-water between the blood and interstitial spaces in the body, and (3) the backward diffusion rate (k_2, per min) of the metabolized ^{15}O-water between the blood and interstitial spaces in the body. The differential equations for the arterial activity concentration of ^{15}O-water at a time t (secs) ($A_w(t)$, Bq/mL), after the physical decay correction can be expressed as follows (Huang *et al*, 1991):

$$\frac{d}{dt}A_w(t) = k \cdot A_o(t) - k_w \cdot A_w(t) + k_2 \cdot C(t) \quad (1a)$$

$$\frac{d}{dt}C(t) = k_w \cdot A_w(t) - k_2 \cdot C(t) \quad (1b)$$

$$A_t(t) = A_o(t) + A_w(t) \quad (1c)$$

where $A_o(t)$ and $A_t(t)$ denote the radioactivity concentration of the arterial $^{15}O_2$ and the total radioactivity from both

Table 1 Variables used in the recirculating water model

Symbol	*Description*	*Unit*
A_o	Radioactivity concentration of arterial $^{15}O_2$	Bq/mL
A_w	Radioactivity concentration of arterial $H_2^{15}O$	Bq/mL
A_t	Total radioactivity concentration from arterial $^{15}O_2$ and $H_2^{15}O$	Bq/mL
A_{plasma}	Radioactivity concentration of arterial plasma	Bq/mL
C	Activity concentration of $H_2^{15}O$ in peripheral tissue in a body	Bq/mL
Fi_{O_2}	Oxygen concentration in inhaled gas	%
Fe_{O_2}	Oxygen concentration in expired gas	%
k	Production rate of recirculating $H_2^{15}O$	per min
k_{BM}	Production rate of recirculating $H_2^{15}O$ obtained from BM approach	per min
k_w	Forward diffusion rate of $H_2^{15}O$ from blood to body interstitial space	per min
k_2	Backward diffusion rate of $H_2^{15}O$ from blood to body interstitial space	per min
λ	Decay constant of ^{15}O (=0.00567 per sec)	per sec
v	Stroke volume	mL
p	k_w/k_2	
r	Respiration rate	per min
R	Fractional water content ratio in whole blood to that in the plasma	
R_{O_2}	Rate of oxidative metabolism in the whole-body system	mL/min
Δt	Delayed appearance time of recirculating water	secs
V_{O_2}	Total volume of molecular oxygen in total blood	mL
V_{TB}	Total volume of blood in a body	mL

$^{15}O_2$ and $H_2^{15}O$, respectively. $C(t)$ is an activity concentration of $H_2^{15}O$ in the peripheral tissue of the total body. Assuming a delayed appearance of RW by Δt (Iida *et al*, 1993), the following equation can be obtained:

$$A_w(t+\Delta t) = k(\alpha_1 \cdot A_t(t) \otimes \exp(-\beta_1 t) + \alpha_2 \cdot A_t(t) \otimes \exp(-\beta_2 t)) \quad (2)$$

where $\otimes$ denotes the convolution integral and:

$$\alpha_{1,2} = \frac{a - 2c \pm \sqrt{a^2 - 4b}}{\pm 2\sqrt{a^2 - 4b}}, \quad \beta_{1,2} = \frac{a \pm \sqrt{a^2 - 4b}}{2},$$
$$a = k + k_w + k_w/p, \quad b = k \cdot k_w/p, \quad c = k_w/p, \quad p = k_w/k_2 \quad (3)$$

Following four approaches were performed to determine the rate constants and $A_w(t)$.

Approach by four parameters fitting: Four parameters, k, Δt, k_w, and p ($=k_w/k_2$), can be determined from the observed RW ($A_w(t)$) and the $A_t(t)$ curves by means of the nonlinear least square fitting (4PF approach).

Approach by one parameter fitting: Once three parameters, Δt, k_w, and p, are fixed by averaging values determined by the 4PF approach, k can then be determined by fitting the Equation 2 to measured $A_w(t)$ from $A_t(t)$ (1PF approach). In this procedure, single datum is sufficient, and thus k can be determined from $A_t(t)$ and the RW counts sampled at a single time point.

Approach from steady-state condition: Similarly to the 1PF procedures, k can be determined from the steady state condition, which is achieved by a continuous administration of $^{15}O_2$ as follows (SS approach). Incorporating the decay constant of ^{15}O ($\lambda = 0.00567$ per secs) into Equations 1a and 1b provides:

$$\frac{d}{dt}A^*_w(t) = k \cdot A^*_o(t) - k_w \cdot A^*_w(t) + k_2 \cdot C^*(t) - \lambda \cdot A^*_w(t) \quad (4a)$$

$$\frac{d}{dt}C^*(t) = k_w \cdot A^*_w(t) - k_2 \cdot C^*(t) - \lambda \cdot C^*(t) \quad (4b)$$

where variables with the symbol * denote that no correction was made for the radioactivity decay of ^{15}O. After continuously administrating $^{15}O_2$, the radioactivity distribution of $A^*_t(t)$, $A^*_w(t)$, and $C^*_t(t)$ reaches a steady state. Thus, the following equations hold:

$$0 = k \cdot A^*_o(t) - k_w A^*_w(t) + k_2 C^*(t) - \lambda A^*_w(t) \quad (5a)$$

$$0 = k_w A^*_w(t) - k_2 C^*(t) - \lambda C^*(t) \quad (5b)$$

Given the values of k_w and k_2 which are determined as averages of 4PF, k can be calculated from the arterial $^{15}O_2$ and $H_2^{15}O$ concentrations at steady state as follows:

$$k = \lambda\left(\frac{k_w + k_2 + \lambda}{k_2 + \lambda}\right)\frac{A^*_w(t)}{A^*_o(t)} \quad (6)$$

Approach by the rate of whole body oxidative metabolism: In this study, an alternative approach is provided to obtain k, from the rate of oxidative metabolism in the whole-body system (BM approach). With this alternative approach, we assume that the production rate of RW or k is proportional to the rate of oxidative metabolism in the whole-body system (i.e., $BMRO_2$ (R_{O_2}, mL/min)). The rate of oxidative metabolism may change dependent on physiologic status of the subject. In addition, we assumed that this index can be defined from the difference of oxygen concentration between inhaled and exhaled trachea air samples. Therefore, the above can be expressed as follows:

$$k = c \cdot \frac{R_{O_2}}{V_{O_2}} \text{ (per min)} \quad (7a)$$

or

$$k_{BM} = \frac{k}{c} = \frac{R_{O_2}}{1.36 \cdot Hb \cdot V_{TB}} \quad (7b)$$

where c is the proportionality constant, k_{BM} the production rate of RW obtained from BM approach, V_{O_2} (mL) the total volume of molecular oxygen in total blood, 1.36 mL/g the amount of oxygen molecules combined with unit mass of hemoglobin, Hb (g/mL) represents the hemoglobin concentration in the arterial blood, and V_{TB} (mL) is the total volume of blood in the body.

Simulation

A series of simulation studies were performed to investigate the effects of errors on estimated $CMRO_2$ value in the model parameters (k, Δt, k_w, and p). In these simulations, a typical arterial blood time activity curve (TAC) of $^{15}O_2$ and $H_2^{15}O$ after DARG protocol (Kudomi *et al*, 2005) obtained in a monkey study was used. RW TACs were generated from the whole blood TAC by assuming baseline values of k as 0.13, 0.11, 0.34, and 0.73 per min, Δt as 20, 11, 5, and 3 secs, k_w as 0.38, 0.43, 0.98, and 0.87 per min, and p as 1.31, 1.01, 0.98, and 0.83, corresponding to humans, pigs, monkeys, and rats, respectively. Tissue TACs were generated by assuming CBF = 50 mL/min per 100 g and OEF = 0.4 ($CMRO_2$ was defined as: $CMRO_2 = CBF \times OEF \times C_aO_2$, where C_aO_2 is the arterial oxygen content. This simulation was intended to investigate magnitude of error as a percentage difference, so that arbitrary value of C_aO_2 was assumed) (Hayashi *et al*, 2003), using a kinetic formula for oxygen and water in the brain tissue (Mintun *et al*, 1984; Shidahara *et al*, 2002; Kudomi *et al*, 2005). $CMRO_2$ values were calculated by the DARG method (Kudomi *et al*, 2005), in which RW TACs were separated from the whole blood by changing k from 0.0 to 1.0 per min, Δt from 0 to 30 secs, k_w from 0.0 to 2.0 per min, and p from 0.0 to 2.0, respectively. Errors in the estimated $CMRO_2$ were presented as a percentage difference from the assumed true values.

Subjects

Subjects consisted of four groups including monkeys, pigs, rats, and clinical patients. Monkeys were six healthy *macaca fascicularis* with body weight of 5.2 ± 0.8 kg and age ranging from 3- to 4-year old. Pigs were three farm pigs

with body weight of 38 ± 9 kg and age from 4 to 12 months. Rats were 12 male Wistar rats with body weight of 300 ± 54 g and age from 7 to 8 weeks. All animals were studied during anesthesia. The animals were maintained and handled in accordance with guidelines for animal research on Human Care and Use of Laboratory Animals (Rockville, National Institute of Health/Office for Protection from Research Risks, 1996). The study protocol was approved by the Subcommittee for Laboratory Animal Welfare of National Cardiovascular Center.

Human data were retrospectively sampled from an existing database at National Cardiovascular Center which documented subjects who underwent PET examination after the ^{15}O-steady-state protocol. There were 231 total samples, with body weight and age ranging from 58 ± 10 kg, and 63 ± 14 years, respectively. Only the arterial $^{15}O_2$ and $H_2^{15}O$ radioactivity concentrations measured at the steady-state condition were used for the present analysis.

Experimental Protocol

The six monkeys were anesthetized using propofol (4 mg/kg/h) and vecuronium (0.05 mg/kg/h) assigned as a baseline in contrast to the after physiologically stimulated conditions. Animals were intubated and their respiration was controlled by an anesthetic ventilator (Cato, Drager, Germany). Each monkey inhaled 2,200 MBq $^{15}O_2$ for 20 secs. After 3 mins, the monkeys were injected with 370 MBq $H_2^{15}O$ for 30 secs by the anterior tibial vein. This was aimed at assessing both CBF and $CMRO_2$ according to the DARG technique (Kudomi *et al*, 2005). At 30 secs before inhaling $^{15}O_2$ to the monkeys, arterial blood was withdrawn from the femoral artery for 420 secs at a rate of 0.45 mL/min using a Harvard pump (Harvard Apparatus, Holliston, MA, USA). The whole blood TAC was measured with a continuous monitoring system (Kudomi *et al*, 2003) and the $A_t(t)$ was obtained. Meanwhile, we also manually obtained 0.5 mL of arterial blood samples from the contralateral femoral artery at 30, 50, 70, 90, 110, 130, 160, 190, and 360 secs after the $^{15}O_2$ inhalation. For the analysis of sampled blood, 0.2 mL of the blood were used for measurement of the radioactivity concentration of the whole blood, and the rest of the blood sampled (~0.3 mL) was immediately centrifuged for separation to measure the plasma radioactivity concentration ($A_{plasma}(t)$, Bq/mL). The radioactivity concentration was measured using a well counter (Molecular Imaging Laboratory Co. Ltd, Suita, Japan).

In two monkeys, anesthetic level was changed by altering the injection dose of propofol from 4 (baseline) to 8 and then to 12 and 16 mg/kg/h in one monkey, and to 5 and then to 7, 10, and 15 mg/kg/h in the other. In another monkey, $PaCO_2$ level was varied from 39 (baseline) to 47, and then to 33, 26, and 42 mm Hg by changing the respiratory rate. Each measurement for $^{15}O_2$ inhalation and $H_2^{15}O$ injection was initiated after at least 30 mins of applying the physiologic stimulation to achieve a steady state. All procedures were the same as those for the baseline, with the exception of the manual blood sample, which was obtained only once at 70 secs.

Before and after 6 mins of the $^{15}O_2$ inhalation, oxygen concentration in both inhaled (Fi_{O_2}, %) and end-tidal expiratory gas (Fe_{O_2}, %) was measured by the anesthetic ventilator in five out of the six monkeys. Using the respiration rate (r, per min) and the stroke volume (v, mL) indicated on the ventilator, the $BMRO_2$ (R_{O_2} mL/min) was calculated using the following equation:

$$R_{O_2} = (Fi_{O_2} - Fe_{O_2}) \cdot v \cdot r.$$

All monkeys received a PET measurement to assess the $CMRO_2$ at physiologically baseline condition. The scan protocol followed the DARG technique (Kudomi *et al*, 2005) in which a 6-mins single dynamic PET scan was performed in conjunction with the administration of dual tracers (i.e., $^{15}O_2$ followed by $H_2^{15}O$ after a 3-mins interval). PET scanner used was ECAT HR (Siemens-CTI, Knoxville, TN, USA), which provided 47 tomographic slice images for an axial field-of-view of approximately 150 mm. We performed arterial–sinus blood sampling to obtain a global OEF (OEF_{A-V}) (A–V difference approach). We sampled 0.2 mL of arterial and sinus blood simultaneously during each PET scan and measured their oxygen content (C_aO_2 and C_vO_2, respectively) (Kudomi *et al*, 2005). The OEF_{A-V} was calculated as: $OEF_{A-V} = (C_aO_2 - C_vO_2)/C_aO_2$.

With regards to the farm pigs involved in this experiment, we used existing data, which were originally obtained in one of the myocardial projects. During the study, three farm pigs were anesthetized. Anesthesia was induced by ketamine (10 mg/kg) and maintained using propofol (4 mg/kg/h). Animals were intubated and their respiration was controlled by the anesthetic ventilator. Venous blood was labeled with $^{15}O_2$ using a small artificial lung unit (Magata *et al*, 2003). $^{15}O_2$-labeled blood (222 to 700 MBq) was injected for 10 secs via anterior tibial vein. At 30 secs before this injection, arterial blood was withdrawn from the femoral artery at a rate of 0.45 mL/min using the Harvard pump and continued for 420 secs. The whole blood TAC ($A_t(t)$) was then measured with a continuous monitoring system (Kudomi *et al*, 2003). Meanwhile, we manually sampled 0.5 mL of arterial blood from the contralateral femoral artery at 30, 60, 90, 90, 120, 180, 240, and 300 secs after the $^{15}O_2$-labeled blood injection. For the analysis of sampled blood, 0.2 mL of the blood were used for measurement of the radioactivity concentration of the whole blood, and the rest of the blood sampled (~0.3 mL) was immediately centrifuged for separation to measure the plasma radioactivity ($A_{plasma}(t)$, Bq/mL). The radioactivity was measured using the well counter.

Data for rats were also originally obtained for other projects, and only the blood counts were used in this study. Anesthesia was induced with pentobarbital (50 mg/kg). A 10 mL of venous blood was labeled $^{15}O_2$ using a small artificial lung unit as described previously (Magata *et al*, 2003), and approximately 1 mL of $^{15}O_2$-labeled blood (37 to 74 MBq) was injected for 30 secs via the tail vein. Arterial blood samples of 0.1 mL each were obtained from the femoral artery at 5-secs intervals for 60 secs and 10-secs intervals for another 60 secs after the injection. Whole blood radioactivity concentration was measured using the well counter to be used as $A_t(t)$. Arterial blood samples of

0.2 mL each were obtained at 30, 60, 90, and 120 secs, and the plasma radioactivity concentration ($A_{plasma}(t)$) was measured by the well counter.

For clinical patients, the blood radioactivity concentration was obtained from previously performed PET examinations, which followed the steady-state protocol (Hirano *et al*, 1994). Each patient inhaled both $^{15}O_2$ and $C^{15}O_2$ to reach the steady state with an inhalation dose of approximately 1,200 and 500 MBq/min, respectively. Five to seven arterial blood samples were obtained during the steady state from the brachial artery. Mean values of radioactivity concentration of the whole blood and plasma, $A_t(t)$ and $A_{plasma}(t)$, respectively, were obtained for both $^{15}O_2$ and $C^{15}O_2$ PET examination.

Data Analysis

Using the blood activity data obtained from monkeys, pigs, and rats at baseline conditions, k as well as Δt, k_w and p were first determined by the 4PF approach, in which Equation 2 was applied to fit the $A_w(t)$ using the observed $A_t(t)$. Because the solubility of the oxygen is negligibly small in the plasma, we assumed that all radioactivity in plasma fraction comes from $H_2^{15}O$ and that the water content ratio of whole blood to plasma (R) does not change during measurement, which means that the kinetics of water molecules immediately reach equilibrium between the plasma and the cellular fraction (Mintun *et al*, 1984; Iida *et al*, 1993). Thus, $A_w(t)$ was obtained from the equation: $A_w(t) = A_{plasma}(t) \cdot R$, where R value was obtained from the sampled blood at the end of the scan (at which all the radioactivity in the blood can be considered as coming from $H_2^{15}O$ because inhaled $^{15}O_2$ is all metabolized).

Given that the values of Δt, k_w, and p were averages determined from 4PF for monkeys, pigs, and rats, only k was determined by fitting Equation 2 to A_w. This was calculated at various points in time, more specifically, in 30, 50, 70, 90, 110, 130, 160, and 190 secs for monkeys, in 30, 60, 90, 90, 120, 180, and 240 secs for pigs, and in 30, 60, 90, and 120 secs for rats. The optimal time point for k under the 1PF approach was determined, so that $(k_{4PF}-k_{1PF})/k_{4PF}$ reaches a minimal value. Here, k_{4PF} and k_{1PF} denote k values determined by the 4PF and 1PF approaches, respectively. The values of k in monkeys at baseline condition, together with those in pigs and rats were compared between 4PF and 1PF approaches, in which a k value from the optimal single time point was used.

In three of the monkeys, which were physiologically stimulated, k of 1PF approach was obtained using single time point of A_w. Assuming the total blood volume (V_{TB}) for monkeys as 360 mL (Lindstedt and Schaeffer, 2002), and using Hb as measured value in each experiment, k_{BM} was calculated from R_{O_2} according to Equation 7b. Then, k_{BM} obtained as: $k_{BM} = 0.00204R_{O_2}$ was compared with k determined by 1PF.

For clinical data obtained from the steady-state (SS approach) PET examinations, Equation 6 was used to determine the k values of the SS approach for each patient, in which values of k_w and k_2 were 0.38 and 0.29 per min as obtained in a previous work by Huang *et al* (1991).

$CMRO_2$ and OEF values in monkeys at baseline condition were calculated using the RW TACs obtained by four different methods (i.e., directly measured $A_w(t)$ ($n = 6$), 4PF ($n = 6$), 1PF ($n = 6$), and BM approaches ($n = 5$)). Regions-of-interest were selected for over the whole brain, and $CMRO_2$ and OEF values were obtained in those regions-of-interest. The $CMRO_2$ values compared among the four methods mentioned above to estimate RW TACs. The Bland–Altman method was applied to analyze the agreement of OEF values between the methods. Also, OEF values were compared with OEF_{A-V}.

All data were presented as mean ± 1 standard deviation. Student's t-test was used and Pearson's regression analysis was applied to compare two variables. A probability value of <0.05 was considered statistically significant.

Results

Figure 1 shows results from the simulation study, and shows the magnitude of errors in $CMRO_2$ calculated by the DARG method as well as errors in the parameters, k, Δt, k_w, and p. Errors in $CMRO_2$ were most sensitive to errors in k amongst all species, namely the production rate constant of RW in the arterial blood. After errors in k, errors in $CMRO_2$ were sensitive to errors in Δt. Errors in k_w and p, however, appeared to cause relatively insignificant errors in $CMRO_2$. More specifically, only 5 to 10% errors are caused in $CMRO_2$ by a change of ± 50% in k_w and p.

Figures 2A–2C show examples of the arterial whole blood curves (A_t) and RW TAC (A_w) observed in typical studies on a monkey, a pig, and a rat, respectively. The RW curves became constant after a period in all species. The rise time or appearance of the RW curves, $A_w(t)$, was significantly delayed compare to that of whole blood curve, $A_t(t)$. $A_w(t)$ curves fitted by 4PF well reproduced the measured RW curves in three species: monkeys, pigs, and rats. Table 2 summarizes values of k, Δt, k_w, and p obtained by the four parameter fitting (4PF approach), at the baseline for monkeys, pigs, and rats, and also k value obtained by the steady-state formula for clinical patients. Those comparisons showed that the k was significantly different among species ($P < 0.001$) except between pig and human subjects, and it was significantly lower in smaller animals. Likewise, Δt showed significant differences among the three species ($P < 0.001$), and it was also lower in smaller animals.

Table 3 summarizes k and $CMRO_2$ values obtained from a series of PET experiments performed on six monkeys at baseline condition, and for increased anesthesia (in two monkeys), and changed $PaCO_2$ levels (in one monkey). The best agreement of k values between 4PF and 1PF approaches was obtained from the blood sample data taken at 60, 70, and 60 secs in pigs, monkeys, and rats, respectively, and was used in the 1PF approach. With this

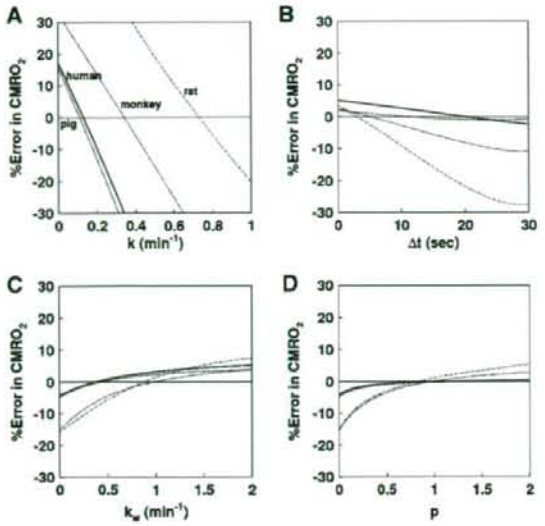

Figure 1 Error in $CMRO_2$ values due to errors in (**A**) k, (**B**) Δt, (**C**) k_w, and (**D**) p for assumed human, pig, monkey and rat. The same type of line indicates the same species. The percentage differences in the $CMRO_2$ values from the assumed true values (Table 1) were plotted as a function of the simulated value of k, Δt, k_w, and p.

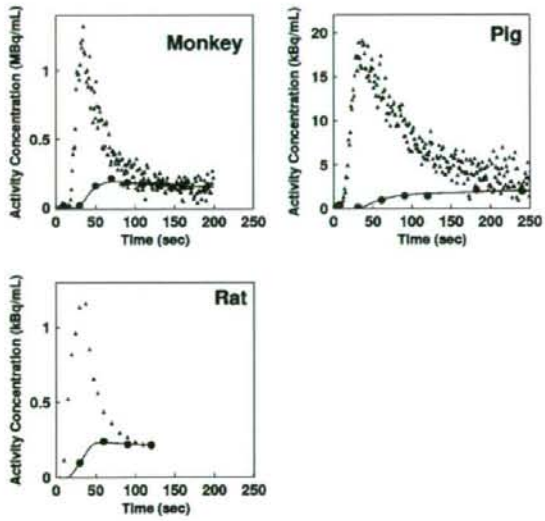

Figure 2 Representative comparison of the measured arterial whole blood and RW time activity curves for monkey, pig, and rat. Closed triangles and closed circles represent the measured whole blood and RW time activity curves, respectively. Estimated time activity curves by 4PF approach were also plotted in a solid line, and indicated a good agreement with the measured one.

optimized calibration protocol, k values were in a good agreement between 4PF and 1PF approaches. As shown in Figure 3, the regression analysis showed significant correlation for 21 animals including 6 monkeys, 3 pigs, and 12 rats ($P<0.001$), and there was no significant difference between the two variables. Figure 4 shows that k values calculated by the 1PF approach (at an optimized time) were in a good agreement with those calculated with the $BMRO_2$. Namely, the regression analysis showed significant correlation ($P<0.001$, $n=16$) and also that there was no significant difference between the two variables. Note that, in the $CMRO_2$ calculation by $BMRO_2$, k values were normalized according to the regression line shown in Figure 4. It should also be noted that calculated $CMRO_2$ values at the baseline shown in Table 3 were not significantly different among the four techniques. The average ($\pm$s.d.) values of obtained OEF were 0.53 ± 0.08, 0.52 ± 0.09, 0.54 ± 0.08, 0.54 ± 0.09, and 0.56 ± 0.04 from A–V difference, directly RW measured approach, 4PF, 1PF, and BM approaches, respectively. The Bland–Altman analysis of OEF values between from A–V difference and from others showed small over/underestimation, that is., with bias $\pm$ s.d. of -0.02 ± 0.09, 0.01 ± 0.07, 0.01 ± 0.08, and 0.02 ± 0.09, by direct RW, 4PF, 1PF, and BM approaches, respectively. Neither of the current methods (direct RW, 4PF, 1PF, and BM) was significantly different from A–V difference approach.

Discussion

Our study showed that the mathematical formula based on the physiologic model that reproduced the time-dependent concentration of RW in the arterial blood after a short-period inhalation of $^{15}O_2$ is indeed adequate. Our approach also simplified the procedures for sequential assessment of RW in $^{15}O_2$ inhalation PET studies, although previous approaches required frequent blood samples and centrifuges of each arterial blood sample. The present approach is an extension of a previous study by Iida *et al* (1993) and Huang *et al* (1991). It is essential if one intends to apply the rapid $^{15}O_2$ PET technique (Kudomi *et al*, 2005) to pharmacologic and physiologic stress studies on a wide range of species. Because the PET acquisition period can be prolonged >3 mins, statistical accuracy can be significantly improved as compared with Ohta *et al* (1992) and other researchers (Fujita *et al*, 1999; Vafaee and Gjedde, 2000; Okazawa *et al*, 2001*a*, *b*; Yamauchi *et al*, 2003; Mintun *et al*, 2002), under which to avoid effects of RW, the data acquisition period was limited only to <3 mins (Meyer *et al*, 1987; Ohta *et al*, 1992).

The present RW formula consists of three rate parameters of the production rate of RW in the arterial blood (k), and the forward and backward diffusion rate constants of RW between the blood and the peripheral tissues. The k was presumed to correspond to the oxygen metabolism in the total body system, $BMRO_2$, and was in fact shown to be

Table 2 Averaged values of k, Δt, k_w, and p for monkeys, pigs, rat, and human subjects under baseline condition

	Weight (kg)	k *(per min)*	*Δt (secs)*	k_w *(per min)*	p
Monkey	5.2 ± 0.8^a	0.34 ± 0.16^a	4.5 ± 1.4^a	0.98 ± 0.48	0.98 ± 0.30
Pig	38 ± 9^a	$0.11 \pm 0.02^{a,b}$	10.8 ± 1.8^a	0.83 ± 0.19	1.01 ± 0.26
Rat	0.30 ± 0.054^a	0.73 ± 0.16^a	2.9 ± 1.7^a	0.87 ± 0.30	0.83 ± 0.32
Human	58 ± 10^a	$0.129 \pm 0.023^{a,b}$	—	—	—

Monkey: $n = 6$; pig: $n = 3$; rat: $n = 12$; and human: $n = 231$. Measured values were obtained by 4PF for monkey, pig, rats, whereas those for human were obtained using data in a steady-state method.

[a]Denotes $P < 0.001$ for other species.

[b]Denotes that the difference was not significant in k between pig and human subjects.

Table 3 Values of k and $CMRO_2$ in the whole brain region for monkeys under physiologically baseline and stimulated conditions

ID	*Condition*	k *(per min)*			*$CMRO_2$ (mL/min per 100 g)*			
		4PF	*1PF*	*$BMRO_2$*	*Reference*	*4PF*	*1PF*	*$BMRO_2$*
1	BL	0.36	0.42	—	3.7	3.7	3.6	—
2	BL	0.62	0.66	1.24	3.0	3.3	3.4	3.4
3	BL	0.32	0.39	0.83	3.0	3.1	3.0	2.9
	(Dose of propofol)							
4	BL	0.21	0.18	0.55	2.0	2.0	2.0	1.8
	8 mg/kg/h	—	0.30	0.69	—	—	—	—
	12 mg/kg/h	—	0.23	0.52	—	—	—	—
	16 mg/kg/h	—	0.16	0.40	—	—	—	—
5	BL	0.12	0.15	0.31	2.1	2.1	2.0	1.8
	5 mg/kg/h	—	0.15	0.32	—	—	—	—
	7 mg/kg/h	—	0.16	0.35	—	—	—	—
	10 mg/kg/h	—	0.18	0.36	—	—	—	—
	15 mg/kg/h	—	0.071	0.29	—	—	—	—
	($PaCO_2$ level)							
6	BL	0.43	0.46	0.95	2.8	3.1	3.0	3.3
	47 mm Hg	—	0.20	0.64	—	—	—	—
	33 mm Hg	—	0.21	0.46	—	—	—	—
	26 mm Hg	—	0.14	0.28	—	—	—	—
	42 mm Hg	—	0.33	0.82	—	—	—	—

4PF, four parameters fitting; 1PF, one parameter fitting; $BMRO_2$, total body metabolic rate of oxygen; BL, baseline condition.
Reference: RW TAC was obtained using measured RW data at a baseline condition in all monkeys ($n = 6$). No statistically significant differences were found in $CMRO_2$ between reference and other techniques.

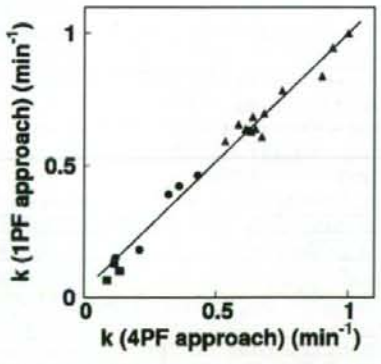

Figure 3 Comparison of the production rates of RW (k, per min) obtained by 4PF and those by 1PF. Squares, circles, and triangles correspond to pigs, monkeys, and rats, respectively. The regression line was $y = 0.97x + 0.026$ (per min) ($r = 0.98$).

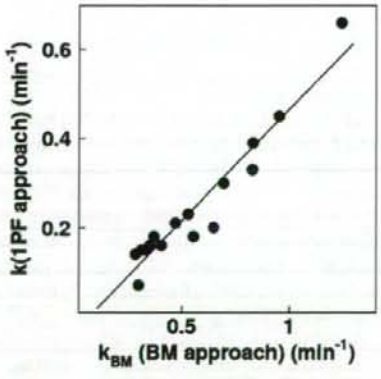

Figure 4 Comparison of the production rates of RW obtained by BM approach and those by 1PF approach in five monkeys at various anesthetic and $PaCO_2$ levels. The regression line was $y = 0.50x - 0.034$ (per min) ($r = 0.95$).

significantly correlated to $BMRO_2$, as measured from the trachea gas sampling (Figure 4). The latter two parameters (k_w and p) appeared to be consistent and did not differ across various species (Table 2). Also, change in those parameters was less sensitive in $CMRO_2$ (Figure 1). These findings suggest that the production of RW after inhalation of $^{15}O_2$ could be described only by a single parameter of k, as shown in Figure 3, although further studies are required to validate this because the method was only tested in a group with small number of subjects of particular physiologic situation (under anesthesia) and has not been applied to different populations. It is also important to note that this parameter (k) estimated from the $BMRO_2$ (i.e., BM approach) provided $CMRO_2$, which was consistent with the trachea gas samplings shown in Figure 4, and that the obtained OEF values by the approaches of 4PF, 1PF, and BM applied in the present study were not significantly different to that by A–V difference approach as revealed by Bland–Altman analysis.

The simulation study also showed that the most sensitive parameter in $CMRO_2$ was the RW production rate constant, k, followed by Δt. It was therefore suggested that k could be determined with a single blood sampling procedure using the 1PF approach, in which other parameter values were determined and fixed from results from the 4PF approach. It was further showed that k could be obtained from the BM approach as determined from oxygen concentration in the expiration gas. Both 1PF and BM approaches appeared to be robustly useful in $^{15}O_2$ PET for assessing quantitative $CMRO_2$ and CBF in clinical studies.

It is important to note that k varies significantly depending on the physiologic status even in the same species, as seen in Figure 4. According to the simulation study in Figure 1, this variation causes nonnegligible errors in $CMRO_2$, if a constant k is used. Changes in k from 0.1 to 0.6 per min causes errors in $CMRO_2$ of $\pm 30\%$ in anesthetized monkeys. Results from clinical studies, however, showed the variation in k being less. As shown in Table 2, k for clinical patients was 0.129 ± 0.023 per min, and the coefficient of variation was approximately 18%. Previous work by Huang *et al* (1991) also showed similar value with comparable variations, namely 0.131 ± 0.026 per min in six human subjects. These variations caused only $\pm 5\%$ errors in $CMRO_2$, according to the simulation shown in Figure 1. The small variation in k in clinical patients is attributed to the fact that all subjects were studied at a relatively stable condition without physiologic stimulation. However, careful attention is needed if one intends to scan the patients whose whole-body oxygen metabolism is largely changed from the baseline condition. For example, during several pharmacologically stressed (Wessen *et al*, 1997; Kaisti *et al*, 2003), exercise-induced physically stressed, and hyper- or hypothermia (Sakoh and Gjedde, 2003) conditions.

The simulation also showed that size of errors in $CMRO_2$ increased in smaller animals, where the value of k was larger. Recently, $CMRO_2$ as well as CBF have been measured in rats using a small animal PET scanner (Magata *et al*, 2003; Yee *et al*, 2006). Magata *et al* performed multiple blood samplings and plasma separation for multiple blood samples to estimate the RW in their experiment involving rats. The procedures were crucial, but have caused serious alterations of physiologic condition in heart pressure and heart rate due to large amount of blood samples for small animals. Our proposed simplified technique for estimating RW from a single blood sample or from $BMRO_2$, is essential for small animals to be able to maintain the physiologic status. The calculation of $CMRO_2$ also requires whole blood arterial TAC, which can be obtained from arterial blood samplings and could change the physiologic condition. However, such blood sampling could also be avoided by an arterial–venous bypass (Weber *et al*, 2002; Laforest *et al*, 2005), by placing a probe in femoral artery (Pain *et al*, 2004), or by a noninvasive method (Yee *et al*, 2006).

Mintun *et al* (1984) has proposed a simple procedure for RW correction based on a linear interpolation for the bolus $^{15}O_2$ inhalation 60-secs PET scan. As shown in Figure 2, the RW curve is not linear particularly in smaller animals, and a systematic error may be caused or scan duration is limited. Ohta *et al* (1992) and other investigators (Ohta *et al*, 1992; Fujita *et al*, 1999; Vafaee and Gjedde, 2000; Okazawa *et al*, 2001*a*, *b*; Yamauchi *et al*, 2003; Mintun *et al*, 2002), however, have used a technique which does not take into account the RW contribution. Only initial short-period data, namely the 3 mins after the bolus inhalation of $^{15}O_2$, were used in their approach, and thus estimated parameters suffered from statistical uncertainties. The present methodology to estimate RW in the arterial blood allows the prolongation of a PET acquisition period. The technique can also be applicable to the recently proposed sequential administration protocol of $^{15}O_2$ followed by $H_2^{15}O$ to estimate $CMRO_2$ and CBF simultaneously from a single session of a PET scan (Kudomi *et al*, 2005). This protocol, however, required a separation of a RW TAC from the whole blood TAC as showed recently (Kudomi *et al*, 2007).

The k_{BM} determined from the total body oxygen metabolism, namely the BM approach, was significantly greater than k obtained by the 4PF or the 1PF approach, by a factor 2, as shown in Figure 4. The reason is not clear, but partly attributed to the limitation of the simplified model. The body system consists of various organs which have different oxygen metabolism along with different circulation systems and with transit times. It is well known that the apparent rate constant defined with a simplified compartmental model could be underestimated as compared with an average of true rate constants, known as heterogeneity effects (Iida *et al*, 1989; Aston *et al*, 2002). This is, however, not essential.

Simply, linear correction could be applied to convert to the apparent k value as has been performed in this study. $CMRO_2$ values calculated using BM approach for the RW separation, were in good agreement with those determined with the direct measurement of RW as shown in Table 3.

The current method with modeling approach and simplified procedure provided consistent results in terms of time-dependent RW component, and consequently metabolic product of $^{15}O_2$ was separated from arterial whole blood for the $CMRO_2$ assessment in PET examination. The modeling approach to separate metabolite from authentic tracer has been showed previously for 6-[^{18}F]fluoro-L-dopa study (fdopa) (Huang *et al*, 1991). We expect that the modeling approach in conjunction with the simplified method showed in our study could be applied for various kinds of tracers, which require the separation of metabolic product such as fdopa. This approach enables us to assess parametric images for those tracers by eliminating the laborious procedures and by avoiding the amount of blood samplings, particularly for smaller animals.

In conclusion, the present RW model was feasible to reproduce RW TAC from a whole radioactivity concentration curve obtained after $^{15}O_2$ inhalation, and for a wide range of species. The simplified procedure to predict the RW TAC is of use to calculate $CMRO_2$ in smaller animals as well as clinical patients.

Acknowledgements

We acknowledge Mr N Ejima for operating the cyclotron and daily maintenance of CTI ECAT HR. We also gratefully thank Ms Atra Ardekani for her invaluable help on preparing the present paper. We also thank the staff of the Investigative Radiology, Research Institute, National Cardiovascular Center, especially, Dr T Inomata, Dr H Jino, Dr N Kawachi, and Dr T Zeniya for their assistance.

References

Aston JA, Cunningham VJ, Asselin MC, Hammers A, Evans AC, Gunn RN (2002) Positron emission tomography partial volume correction: estimation and algorithms. *J Cereb Blood Flow Metab* 22:1019–34

Eriksson L, Holte S, Bohm Chr, Kesselberg M, Hovander B (1988) Automated blood sampling system for positron emission tomography. *IEEE Trans Nucl Sci* 35:703–7

Eriksson L, Kanno I (1991) Blood sampling devices and measurements. *Med Prog Technol* 17:249–57

Fujita H, Kuwabara H, Reutens DC, Gjedde A (1999) Oxygen consumption of cerebral cortex fails to increase during continued vibrotactile stimulation. *J Cereb Blood Flow Metab* 19:266–71

Hayashi T, Watabe H, Kudomi N, Kim KM, Enmi J, Hayashida K, Iida H (2003) A theoretical model of oxygen delivery and metabolism for physiologic interpretation of quantitative cerebral blood flow and metabolic rate of oxygen. *J Cereb Blood Flow Metab* 23:1314–23

Hirano T, Minematsu K, Hasegawa Y, Tanaka Y, Hayashida K, Yamaguchi T (1994) Acetazolamide reactivity on ^{123}I-IMP single photon emission computed tomography in patients with major cerebral artery occlusive disease: correlation with positron emission tomography parameters. *J Cereb Blood Flow Metab* 14:763–70

Holden JE, Eriksson L, Roland PE, Stone-Elander S, Widen L, Kesselberg M (1988) Direct comparison of single-scan autoradiographic with multiple-scan least-squares fitting approaches to PET $CMRO_2$ estimation. *J Cereb Blood Flow Metab* 8:671–80

Huang SC, Barrio JR, Yu DC, Chen B, Grafton S, Melega WP, Hoffman JM, Satyamurthy N, Mazziotta JC, Phelps ME (1991) Modelling approach for separating blood time-activity curves in positron emission tomographic studies. *Phys Med Biol* 36:749–61

Iida H, Jones T, Miura S (1993) Modeling approach to eliminate the need to separate arterial plasma in oxygen-15 inhalation positron emission tomography. *J Nucl Med* 34:1333–40

Iida H, Kanno I, Miura S, Murakami M, Takahashi K, Uemura K (1989) A determination of the regional brain/blood partition coefficient of water using dynamic positron emission tomography. *J Cereb Blood Flow Metab* 9:874–85

Kaisti KK, Langsjo JW, Aalto S, Oikonen V, Sipila H, Teras M, Hinkka S, Metsahonkala L, Scheinin H (2003) Effects of sevoflurane, propofol, and adjunct nitrous oxide on regional cerebral blood flow, oxygen consumption, and blood volume in humans. *Anesthesiology* 99:603–13

Kudomi N, Choi C, Watabe H, Kim KM, Shidahara M, Ogawa M, Teramoto N, Sakamoto E, Iida H (2003) Development of a GSO detector assembly for a continuous blood sampling system. *IEEE Trans Nucl Sci* 50:70–3

Kudomi N, Hayashi T, Teramoto N, Watabe H, Kawachi N, Ohta Y, Kim KM, Iida H (2005) Rapid quantitative measurement of $CMRO_2$ and CBF by dual administration of ^{15}O-labeled oxygen and water during a single PET scan—a validation study and error analysis in anesthetized monkeys. *J Cereb Blood Flow Metab* 25:1209–24

Kudomi N, Watabe H, Hayashi T, Iida H (2007) Separation of input function for rapid measurement of quantitative $CMRO_2$ and CBF in a single PET scan with a dual tracer administration method. *Phys Med Biol* 52: 1893–908

Laforest R, Sharp TL, Engelbach JA, Fettig NM, Herrero P, Kim J, Lewis JS, Rowland DJ, Tai YC, Welch MJ (2005) Measurement of input functions in rodents: challenges and solutions. *Nucl Med Biol* 32:679–85

Lindstedt L, Schaeffer PJ (2002) Use of allometry in predicting anatomical and physiological parameters of mammals. *Lab Anim* 36:1–19

Magata Y, Temma T, Iida H, Ogawa M, Mukai T, Iida Y, Morimoto T, Konishi J, Saji H (2003) Development of injectable O-15 oxygen and estimation of rat OEF. *J Cereb Blood Flow Metab* 23:671–6

Meyer E, Tyler JL, Thompson CJ, Redies C, Diksic M, Hakim AM (1987) Estimation of cerebral oxygen utilization rate by single-bolus 15O2 inhalation and dynamic positron emission tomography. *J Cereb Blood Flow Metab* 7:403–14

Mintun MA, Raichle ME, Martin WR, Herscovitch P (1984) Brain oxygen utilization measured with O-15 radio-

tracers and positron emission tomography. *J Nucl Med* 25:177–87

Mintun MA, Vlassenko AG, Shulman GL, Snyder AZ (2002) Time-related increase of oxygen utilization in continuously activated human visual cortex. *Neuroimage* 16:531–7

Ohta S, Meyer E, Thompson CJ, Gjedde A (1992) Oxygen consumption of the living human brain measured after a single inhalation of positron emitting oxygen. *J Cereb Blood Flow Metab* 12:179–92

Okazawa H, Yamauchi H, Sugimoto K, Takahashi M, Toyoda H, Kishibe Y, Shio H (2001*a*) Quantitative comparison of the bolus and steady-state methods for measurement of cerebral perfusion and oxygen metabolism: positron emission tomography study using 15O-gas and water. *J Cereb Blood Flow Metab* 21:793–803

Okazawa H, Yamauchi H, Sugimoto K, Toyoda H, Kishibe Y, Takahashi M (2001*b*) Effects of acetazolamide on cerebral blood flow, blood volume, and oxygen metabolism: a positron emission tomography study with healthy volunteers. *J Cereb Blood Flow Metab* 21:1472–9

Pain F, Laniece P, Mastrippolito R, Gervais P, Hantraye P, Besret L (2004) Arterial input function measurement without blood sampling using a beta-microprobe in rats. *J Nucl Med* 45:1577–82

Sakoh M, Gjedde A (2003) Neuroprotection in hypothermia linked to redistribution of oxygen in brain. *Am J Physiol Heart Circ Physiol* 285:H17–25

Shidahara M, Watabe H, Kim KM, Oka H, Sago M, Hayashi T, Miyake Y, Ishida Y, Hayashida K, Nakamura T, Iida H (2002) Evaluation of a commercial PET tomograph-based system for the quantitative assessment of rCBF, rOEF and rCMRO2 by using sequential administration of 15O-labeled compounds. *Ann Nucl Med* 16:317–27

Temma T, Magata Y, Kuge Y, Shimonaka S, Sano K, Katada Y, Kawashima H, Mukai T, Watabe H, Iida H, Saji H (2006) Estimation of oxygen metabolism in a rat model of permanent ischemia using positron emission tomography with injectable ^{15}O-O_2. *J Cereb Blood Flow Metab* 26:1577–83

Vafaee MS, Gjedde A (2000) Model of blood-brain transfer of oxygen explains nonlinear flow-metabolism coupling during stimulation of visual cortex. *J Cereb Blood Flow Metab* 20:747–54

Votaw JR, Shulman SD (1998) Performance evaluation of the Pico-Count flow-through detector for use in cerebral blood flow PET studies. *J Nucl Med* 39:509–15

Weber B, Burger C, Biro P, Buck A (2002) A femoral arteriovenous shunt facilitates arterial whole blood sampling in animals. *Eur J Nucl Med Mol Imaging* 29: 319–23

Wessen A, Widman M, Andersson J, Hartvig P, Valind S, Hetta J, Langstrom B (1997) A positron emission tomography study of cerebral blood flow and oxygen metabolism in healthy male volunteers anaesthetized with eltanolone. *Acta Anaesthesiol Scand* 41:1204–12

Yamauchi H, Okazawa H, Kishibe Y, Sugimoto K, Takahashi M (2003) The effect of acetazolamide on the changes of cerebral blood flow and oxygen metabolism during visual stimulation. *Neuroimage* 20:543–9

Yee SH, Lee K, Jerabek PA, Fox PT (2006) Quantitative measurement of oxygen metabolic rate in the rat brain using microPET imaging of briefly inhaled 15O-labelled oxygen gas. *Nucl Med Commun* 27:573–81

Ann Nucl Med (2008) 22:667–675
DOI 10.1007/s12149-008-0157-9

ORIGINAL ARTICLE

Optimal scan time of oxygen-15-labeled gas inhalation autoradiographic method for measurement of cerebral oxygen extraction fraction and cerebral oxygen metabolic rate

Miho Shidahara · Hiroshi Watabe · Kyeong Min Kim
Nobuyuki Kudomi · Hiroshi Ito · Hidehiro Iida

Received: 7 March 2008 / Accepted: 1 May 2008
© The Japanese Society of Nuclear Medicine 2008

Abstract
Objective Regional cerebral blood flow (CBF), cerebral blood volume, oxygen extraction fraction (OEF), and cerebral metabolic rate of oxygen ($CMRO_2$) can be estimated from $C^{15}O$, $H_2{}^{15}O$, and $^{15}O_2$ tracers and positron emission tomography (PET) using an autoradiographic (ARG) method. Our objective in this study was to optimize the scan time for $^{15}O_2$ gas study for accurate estimation of OEF and $CMRO_2$.
Methods We evaluated statistical noise in OEF by varying the scan time and error caused by the tissue heterogeneity in estimated OEF and $CMRO_2$ using computer simulations. The characteristics of statistical noise were investigated by signal-to-noise (S/N) ratio from repeated tissue time activity curves with noise, which were generated using measured averaged arterial input function and assuming CBF = 20, 50, and 80 (ml/100 g per minute). Error caused by tissue heterogeneity was also investigated by estimated OEF and $CMRO_2$ from tissue time activity curve with mixture of gray and white matter varying fraction of mixture. In the simulations, three conditions were assumed (i) CBF in gray and white matter (CBF^g and CBF^w) was 80 and 20, OEF in gray and white matter (E^g and E^w) was 0.4 and 0.3, (ii) CBF^g and CBF^w decreased by 50%, and E^g and E^w increased by 50% when compared with conditions (i) and (iii). CBF^g and CBF^w decreased by 80%, and E^g and E^w increased by 50% when compared with condition (i).
Results The longer scan time produced the better S/N ratio of estimated OEF value from three CBF values (20, 50, and 80). Errors of estimated OEF for three conditions owing to tissue heterogeneity decreased, as scan time took longer. Meanwhile in the case of $CMRO_2$, 3 min of scan time was desirable.
Conclusions The optimal scan time of $^{15}O_2$ inhalation study with the ARG method was concluded to be 3 min from taking into account for maintaining the S/N ratio and the quantification of accurate OEF and $CMRO_2$.

Keywords O-15 oxygen gas · Positron emission tomography · Autoradiographic method

M. Shidahara (✉) · H. Ito
Molecular Imaging Center, National Institute of Radiological Sciences, 4-9-1 Anagawa, Inage-ku, Chiba 263-8555, Japan
e-mail: sidahara@nirs.go.jp

H. Watabe · K.M. Kim · N. Kudomi · H. Iida
Department of Investigative Radiology, National Cardiovascular Center Research Institute, Osaka, Japan

Introduction

Quantitative cerebral oxygen extraction fraction (OEF) and cerebral metabolic rate of oxygen ($CMRO_2$) images can be measured by oxygen-15-labeled gas ($^{15}O_2$) and positron emission tomography (PET). These physiological parameters have provided important hemodynamic information for the diagnoses of cerebrovascular disease, especially in the case of misery perfusion [1–3]. For effective application of these parameters to urgent clinical study, a simplified diagnostic method to shorten scan time is strongly required and yet retaining the quantification. When compared with the steady-state method, the autoradiographic (ARG) method [4] has the potential to shorten the length of study [5]. A 3-min scan duration following $^{15}O_2$ inhalation has been used by Hatazawa et al. [6]; however, earlier no systematic investigation of optimization of scan time for $^{15}O_2$ study with the ARG method was performed. In this article, by focusing on two factors, namely, signal-to-noise (S/N) ratio on the

functional images and the tissue heterogeneity, the optimal scan duration for the ARG method with $^{15}O_2$ gas was investigated.

Variance of pixel counts in reconstructed image is delivered from randomly emitted and detected photon counts and then propagates to estimated OEF and $CMRO_2$ value. The short physical half-life (about 2 min) of ^{15}O causes large variance of the pixel counts, and, therefore, alternation of the scan duration leads to substantial change on the image quality of PET image, such as S/N ratio.

The influence of tissue heterogeneity on estimated physiological parameters has been reported by several authors [7, 8], and estimation error of cerebral blood flow (CBF) is caused by the assumption that there is only single-tissue CBF in mixed region of gray and white matter, even though different tissues own different CBF values. An optimization scheme of measurement of CBF was provided by Kanno et al. [7, 9], and that study showed the error of estimated CBF from tissue heterogeneity depended on scan time [9]. The effect of tissue heterogeneity in systematic error of OEF has been also analyzed for the steady-state method [10, 11]. However, in the case of the estimation of OEF and $CMRO_2$ with the ARG method and bolus inhalation of $^{15}O_2$, the effects of tissue heterogeneity in $^{15}O_2$ study and the effect of the error in CBF owing to tissue heterogeneity propagates to OEF and $CMRO_2$ estimates are unknown.

In this article, we performed computer simulations of the ARG method with ^{15}O water and $^{15}O_2$ gas under three clinical conditions, namely, normal, misery perfusion, and occlusion. We investigated the relationship between scan time and S/N ratio of estimated OEF. Furthermore, the relationship between scan time and the accuracy in estimated OEF and $CMRO_2$ affected by tissue heterogeneity for both ^{15}O water and $^{15}O_2$ gas studies was examined. By these results, optimized scan time for $^{15}O_2$ gas inhalation protocol was determined especially for clinical application such as ischemic disease.

Materials and methods

Computing CBF, OEF, and $CMRO_2$ using the ARG method

In the ARG method, CBF (ml/g per minute) is computed by a single-tissue compartment model described as follows:

$$\int_0^T C_t^{\mathrm{W}}(t)\mathrm{d}t = \rho_b \int_0^T \mathrm{CBF}\cdot A(t)\otimes \mathrm{e}^{-\rho_b \frac{\mathrm{CBF}}{p}}\,\mathrm{d}t \qquad (1)$$

where $C_t^{\mathrm{W}}(t)$ (cps/ml) is the radioactivity concentration of $H_2{}^{15}O$ study at time t measured by PET (integrated from time 0 to time T), ρ_b is the density of brain tissue (1.04) (g/ml), $A(t)$ (cps/ml) is arterial input function of $H_2{}^{15}O$ at time t measured by the external radiation detector, and p is the partition coefficient factor (fixed as 0.8 ml/ml) [12]. The CBF value for each pixel is estimated in the look-up table manner with observer PET data $\int_0^T C_t^{\mathrm{W}}(t)\mathrm{d}t$ against $\rho_b \int_0^T \mathrm{CBF}\cdot A(t)\otimes \mathrm{e}^{-\rho_b \frac{\mathrm{CBF}}{p}}\,\mathrm{d}t$.

Using the ARG method, OEF and $CMRO_2$ are computed owing to a model by Mintun et al. [4] described as follows:

$$\begin{aligned}\int_0^T C_t^{\mathrm{O}}(t)\mathrm{d}t = {} & \rho_b \int_0^T \mathrm{CBF}\cdot A_{\mathrm{H_2O}}(t)\otimes \mathrm{e}^{-\rho_b \frac{\mathrm{CBF}}{p}} \\ & + \mathrm{OEF}\cdot \mathrm{CBF}\cdot A_{\mathrm{O_2}}(t)\otimes \mathrm{e}^{-\rho_b \frac{\mathrm{CBF}}{p}t} \\ & + \mathrm{CBV}\cdot \mathrm{VR}\cdot(1-\mathrm{OEF}\cdot \mathrm{FV})\cdot A_{\mathrm{O_2}}(t)\mathrm{d}t \end{aligned} \qquad (2)$$

where $C_t^{\mathrm{O}}(t)$ (cps/ml) is the radioactivity concentration of $^{15}O_2$ study at time t measured by PET (integrated from time 0 to time T), CBF (ml/g per minute) values are obtained from $H_2{}^{15}O$ study using Eq. 1, $A_{\mathrm{H_2O}}(t)$ (cps/ml) and $A_{\mathrm{O_2}}(t)$ (cps/ml) are the arterial input functions for $H_2{}^{15}O$ and $^{15}O_2$ components at time t measured by the external radiation detector. CBV is the cerebral blood volume and calculated by the additional PET scan with $C^{15}O$. VR is the small- to large-vessel hematocrit ratio (fixed as 0.85), FV is the effective venous fraction (fixed as 0.835) [4]. OEF is computed from the arterial input functions of $A_{\mathrm{H_2O}}(t)$ and $A_{\mathrm{O_2}}(t)$ and fixed values for p, VR and FV by the look-up table manner in the pixel-by-pixel basis. $CMRO_2$ is then calculated as follows:

$$\mathrm{CMRO_2} = \mathrm{CBF}\cdot \mathrm{OEF}\cdot [\mathrm{O_2}]_a \qquad (3)$$

where $[O_2]_a$ is the arterial oxygen concentration which is given as follows:

$$[\mathrm{O_2}]_a = 1.39\cdot \mathrm{Hb}\cdot \%\mathrm{Sat} \qquad (4)$$

where 1.39 is the averaged oxygen volume associated with a single hemoglobin molecule, Hb is the hemoglobin concentration (g hemoglobin/ml blood), and %Sat is the percentage of saturation in O_2 of the arterial blood.

PET study

To compute CBF, OEF, and $CMRO_2$ images, three PET scans with $C^{15}O$ gas, ^{15}O water, and $^{15}O_2$ gas are required with additional transmission scan. The typical clinical

protocol in National Cardiovascular Center Hospital is as follows:

1. Ten-minute transmission scan with ^{68}Ge–^{68}Ga source.
2. The subject was made to inhale C^{15}O (2.19 MBq per minute) for 1 min and 4 min after the start of the inhalation; PET scan is started for 4 min.
3. The subject is intravenously (right bronchial vein) administered $H_2{}^{15}O$ (0.81 MBq for 20 s bolus injection). PET scan (12 × 5 s, 2 × 15 s total 1.5 min) is started 10 s later from the start of infusion of $H_2{}^{15}O$.
4. The subject was made to inhale $^{15}O_2$ gas (2.19 MBq/min) for 1 min. PET scan (12 × 5 s, 8 × 15 s total 3 min) is started at the same time of the inhalation.

Positron emission tomography scanner is ECAT EXACT 47 (CTI, Knoxville, TN, USA), and all scans are performed with 2D mode (septa extended). For the present study, scan protocol of $^{15}O_2$ gas was extended from conventional 180 s to 300 s (12 × 5 s, 8 × 15 s, and 4 × 30 s).

For the simulations studies, arterial input functions of $A_{H_2O}(t)$ and $A_{O_2}(t)$ in Eq. 2 were mimicked from averaged whole-blood arterial input function of five healthy volunteers (all subjects were men, and mean age was 24.7 ± 3.6 years) [13]. Delay- and dispersion-corrected arterial input functions of the five subjects were averaged and separated into two-component, oxygen-gas, and metabolized water by convolution formula [14] (Fig. 1).

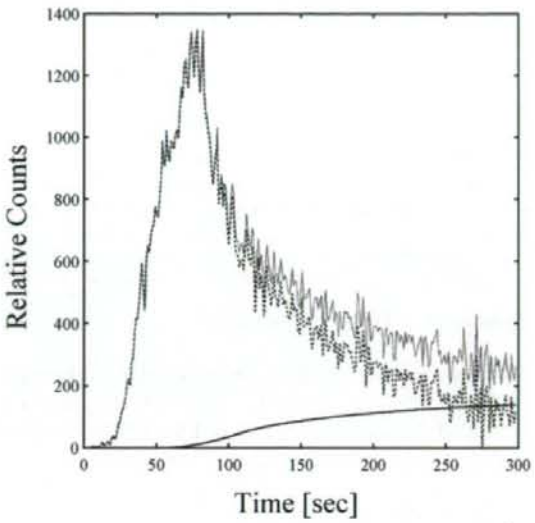

Fig. 1 Delay- and dispersion-corrected arterial input function: whole-blood curve [function: whole-blood curve (*solid line*), O_2 components (*dotted line*), and metabolized water components (*bold solid line*)]

Simulation studies

Two simulation studies were performed.

Simulation 1: S/N ratio in quantitative OEF images

The relationship between the scan duration and statistical noise of OEF values was investigated in terms of S/N ratio. The variance of PET data C_{PET} at frame i was estimated using the following equation [15, 16]:

$$\frac{\sigma(i)}{C_{PET}(i)} = \frac{c}{\sqrt{NEC(i)}} \quad (5)$$

where $\sigma(i)$ is standard deviation (SD) of C_{PET} at frame i and NEC(i) is noise equivalent count [17] at frame i. c is constant factor. To determine c, phantom experiments were performed. A cylindrical phantom (16 cm in diameter and an axial length of 20 cm) filled with water was used for the measurement of statistical noise on reconstructed image. ^{15}O water solution (half-life is 2.04 min, 518 MBq at scan start) was injected in the phantom. Single-PET scanning with dynamic acquisition was performed to obtain 20 frames, each with duration of 60 s. Count rates of true coincidents and random coincidents detected by PET gantry were also recorded, and NEC for each frame was computed. Image reconstruction was performed by direct Fourier transform algorithm with 6.0 mm full width half maximum Gaussian filter that is used for the clinical routine. From each frame data, mean $C_{PET}(i)$ with $\sigma(i)$ were computed from all pixels inside the drawn circular ROI (10 cm in diameter) on the reconstructed image. The constant c was estimated by these data to fit Eq. 5.

To simulate the S/N ratio in the clinical PET study, NEC(i) during PET acquisition was measured in actual PET studies with $^{15}O_2$ gas for five normal volunteers described in earlier section and the averaged $NEC(i)$ data were used in the simulation; 500 noisy simulated PET data, $C^j_{PET}(i)$ ($j = 1, \ldots, 500$) were generated according to Eqs. 2 and 5 under the conditions of CBF = 20, 50, and 80 (ml/100 g per minute) and OEF = 0.2, 0.4, and 0.8. The integration time T in Eq. 2 was set to 60 s, 120 s, 180 s, 240 s, and 300 s and at each integration time T, $OEF^j(T)$ was estimated from each $\int_0^T C^j_{PET}(i)di$ using the ARG method. The S/N ratios at time T were derived from the division of mean estimated OEF(T) using 500 data sets by its SD.

Table 1 Predefined parameters for simulations of tissue heterogeneity

Condition	CBF^g (ml/100 g per minute)	CBF^w (ml/100 g per minute)	OEF^g	OEF^w
(i) Normal	80	20	0.4	0.3
(ii) Misery perfusion	40	10	0.6	0.45
(iii) Occlusion	16	4	0.6	0.45

Three conditions of (i) normal, (ii) misery perfusion, and (iii) occlusion were considered. Cerebral blood flow (CBF) in gray matter (CBF^g) and white matter (CBF^w), and oxygen extraction fraction (OEF) in gray matter (OEF^g) and white matter (OEF^w) were defined

Simulation 2: Tissue heterogeneity

The time dependency of quantitative error in estimated OEF and $CMRO_2$ caused by tissue heterogeneity was evaluated. We assumed that tissue TAC $C_t^m(t)$ in a mixed region of gray and white matter is expressed as

$$C_t^m(t) = \alpha \cdot C_t^g(t) + (1 - \alpha) \cdot C_t^w(t) \quad (6)$$

where α is the fraction of gray matter volume ranged from 0 to 1, and $C_t^g(t)$ and $C_t^w(t)$ are calculated tissue TACs in gray and white matter from Eqs. 1 and 2 with fixed parameters, respectively. In view of the clinical application for ischemic disease, three physiological conditions of (i) normal, (ii) misery perfusion, and (iii) occlusion were considered in the present simulations. CBF in gray matter and white matter, and OEF in gray matter and white matter were defined as shown in Table 1. CBF^m, OEF^m, and $CMRO_2^m$, including the effect of tissue heterogeneity was estimated by the ARG method with the integration time T of 90 s in $H_2{}^{15}O$ study and T = 120 s, 180 s, 240 s, and 300 s in $^{15}O_2$ study.

The magnitude of error in estimated CBF^m value at fixed scanning time of 90 s

Varying the fraction of gray volume [0 : 1], CBF^m of three conditions in (i), (ii), and (iii) was estimated by the ARG method and the differences between CBF^m and ideal CBF value CBF_{ave} in Eq. 7 were compared.

$$CBF_{ave} = \alpha \cdot CBF_g + (1 - \alpha) \cdot CBF_w \quad (7)$$

Time dependency of estimated OEF^m from CBF^m

For three conditions, $OEF^m(T)$ and $CMRO_2^m(T)$ at integration time T (= 120 s, 180 s, 240 s, and 300 s) were estimated using CBF^m value and the ARG method. Varying the fraction of gray volume [0:1] for $H_2{}^{15}O$ and $^{15}O_2$ study, OEF^m and $CMRO_2^m$ were compared with ideal OEF and $CMRO_2$ values (OEF_{ave} and $CMRO_{2ave}$), shown in Eq. 8:

$$OEF_{ave} = \alpha \cdot OEF^g + (1 - \alpha) \cdot OEF^w$$
$$CMRO_{2ave} = \alpha \cdot CMRO_2{}^g + (1 - \alpha) \cdot CMRO_2{}^w \quad (8)$$

In the calculations of $CMRO_2^m$, CBF^m values were employed.

Results

Simulation 1: S/N ratio in quantitative OEF images

Figure 2a shows the relationship between NEC and coefficient of variance (COV) which is defined as the ratio between SD of C_{PET} and C_{PET}. Constant factor c in Eq. 5 was estimated from the relationship using the least-squares fitting and resulted in 38.1 (r = 0.996). Figure 2b shows averaged NEC curve of 5 $^{15}O_2$ studies.

Oxygen extraction fraction under the condition of CBF = 20, 50, and 80 (ml/100 g per minute) was estimated using noise-added time activity curve (Fig. 3a) using calculated $\sigma(i)$ in Eq. 5 and averaged NEC curve. Figure 3 shows the relationship between integrated time T and S/N ratio in estimated OEF values [OEF = 0.4 (Fig. 3b), OEF = 0.2 (Fig. 3c), and OEF = 0.6 (Fig. 3d)]. In general, the longer scan time provided better S/N ratio as shown in Fig. 3. In the case of low OEF (i.e., OEF = 0.2), S/N ratio reached plateau more rapidly than other cases.

Actual OEF and $CMRO_2$ images computed by the ARG method with T = 60 s, 180 s for a young normal volunteer were shown in Fig. 4. Less statistical noise in both OEF and $CMRO_2$ images with T = 180 s was visually observed when compared with T = 60 s. This figure supports the simulation results.

Simulation 2: Tissue heterogeneity

The relationship between the error of estimated CBF^m for $H_2{}^{15}O$ study and the fraction of gray volume is shown in Fig. 5. Lower CBF values in both gray and white matters [i.e., condition (ii) CBF^g = 40, CBF^w = 10, or condition (iii) CBF^g = 16, CBF^w = 4] reduce the error of

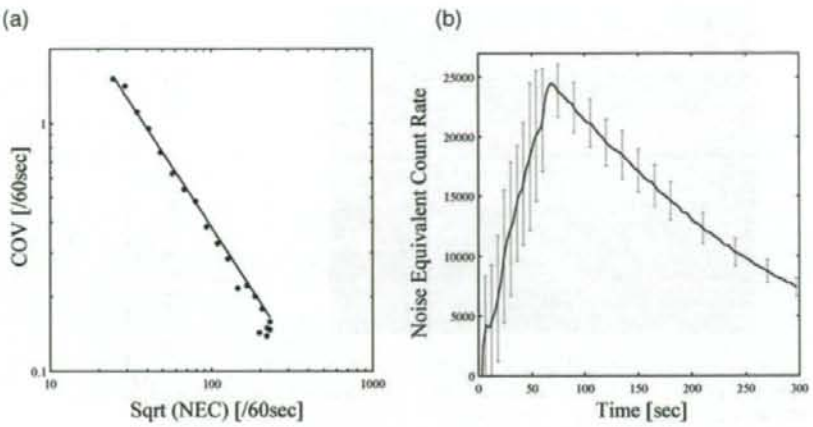

Fig. 2 **a** The relationship between noise equivalent count (NEC) and coefficient of variance (COV) obtained from phantom experiment with ECAT EXACT. **b** Averaged dynamic NEC curve with standard deviation of $^{15}O_2$ study among five volunteers

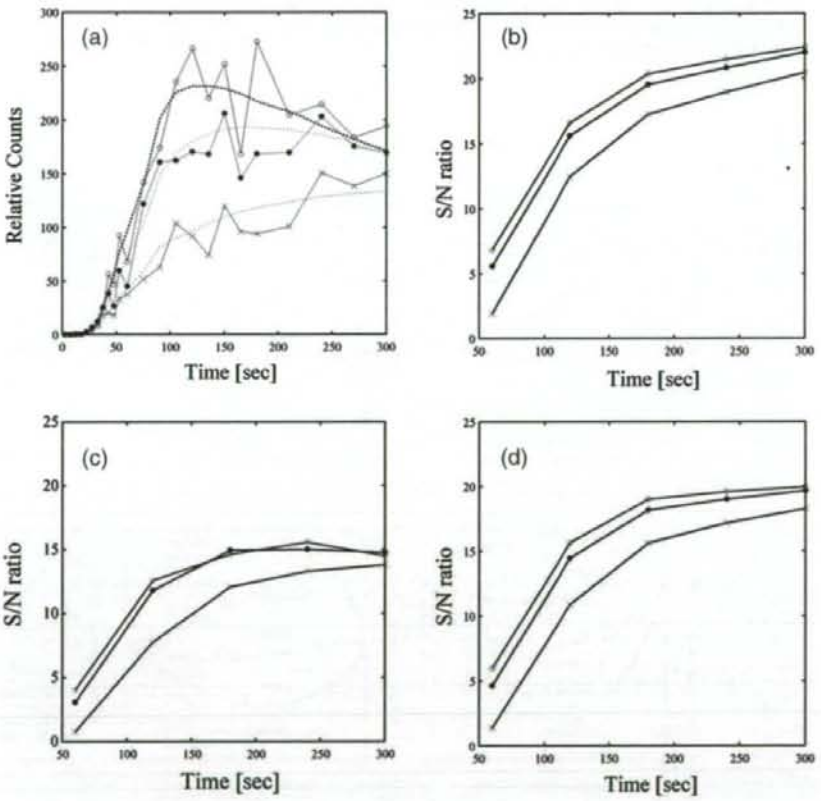

Fig. 3 **a** Noise-added time activity curves of $^{15}O_2$ study assuming oxygen extraction fraction (OEF) = 0.4 and cerebral blood flow (CBF) = 80 (*open circle*), 50 (*closed circle*), and 20 (*cross*; ml/100 g per minute), and true time activity curves (*dotted lines*). Time dependency of signal-to-noise ratio in estimated (**b**) OEF = 0.4, (**c**) OEF = 0.2, and (**d**) OEF = 0.6 using CBF = 80 (*open circle*), 50 (*closed circle*), and 20 (*cross*; ml/100 g per minute)

estimated CBF^m when compared with condition (i) $CBF^g = 80$, $CBF^w = 20$. The maximum error of CBF^m with three conditions of (i) normal, (ii) misery perfusion, and (iii) occlusion were −12.5% (α = 0.39), −6.7% (α = 0.38), and −2.8% (α = 0.35), respectively.

Figures 6 and 7 show the relationship between the error of estimated $OEF^m(T)$ (a) and $CMRO_2^m(T)$ (b) and the relationship between the maximum error and scanning time. As shown in Fig. 7a, b, by increasing integration time, the error of estimated OEF^m and

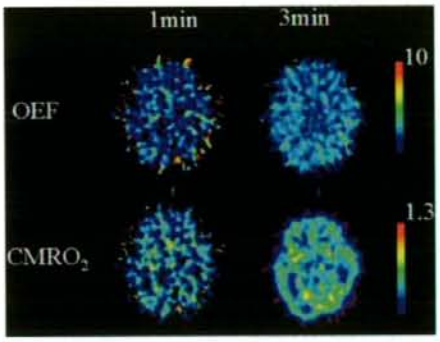

Fig. 4 An example of clinical images of OEF and cerebral metabolic rate of oxygen ($CMRO_2$) obtained from $T = 60$ s and 180 s scan time for a patient. Image reconstruction was performed with direct Fourier transform algorithm with 6 mm Gaussian filter. Reconstructed image has 128 × 128 × 47 slices with 1.84 mm × 1.84 mm and 3.38 mm pixel sizes. Attenuation correction using transmission data and scatter correction with the deconvolution scatter function were applied

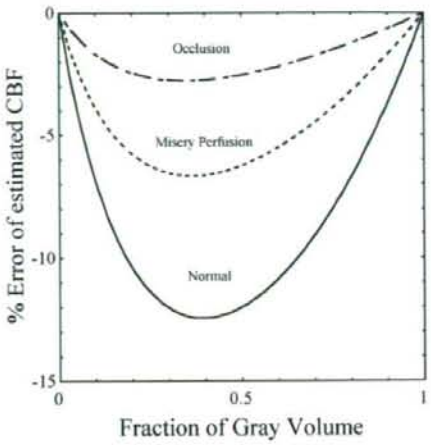

Fig. 5 The effect of tissue heterogeneity on % error of CBF^m in $CBF^s = 80$, $CBF^n = 20$ (*solid line*), $CBF^s = 50$, $CBF^n = 12$ (*dotted line*), and $CBF^s = 16$, $CBF^n = 4$ (*dotted dashed line*)

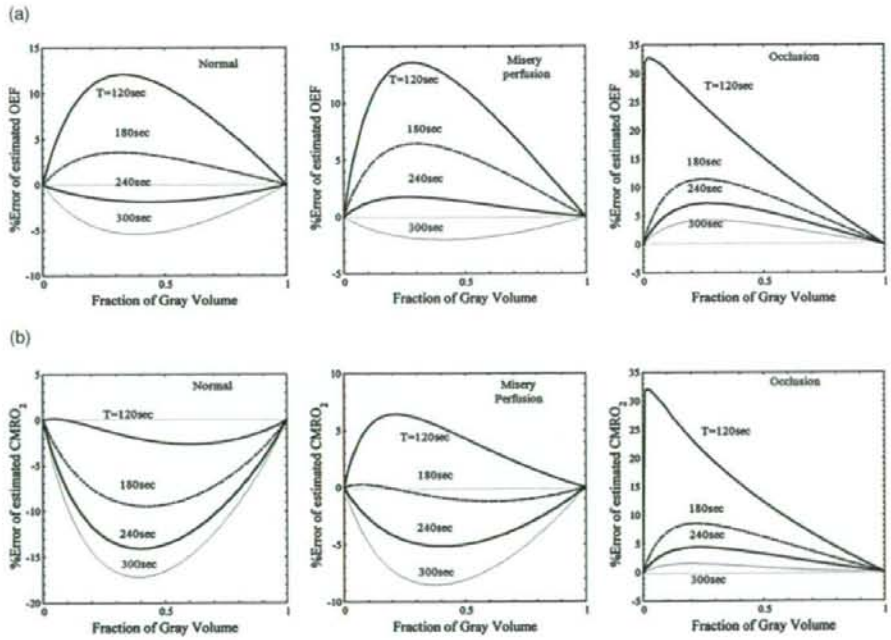

Fig. 6 The effect of tissue heterogeneity on % error of OEF^m (T) (**a**) and $CMRO_2^m$ (T) (**b**) in normal, misery perfusion, and occlusion conditions for integration times of 120 s, 180 s, 240 s, and 300 s including the effect of tissue heterogeneity in $H_2{}^{15}O$ study

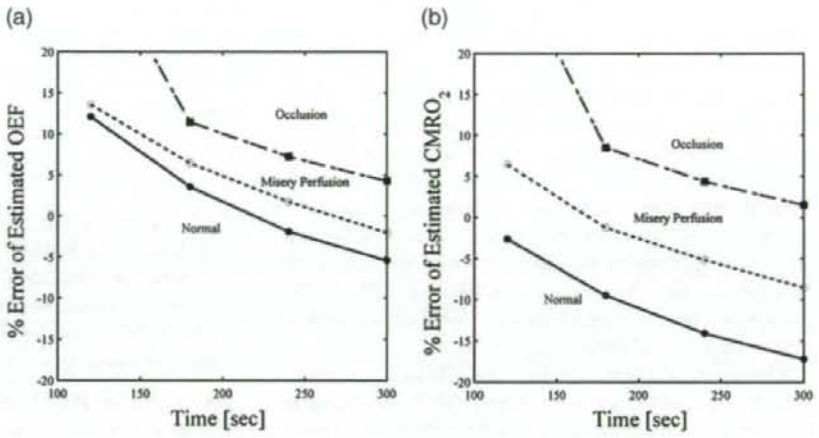

Fig. 7 The maximum error of estimated OEF^m (T) (**a**) and $CMRO_2^m$ (T) (**b**) for integration times of 120 s, 180 s, 240 s, and 300 s including the effect of tissue heterogeneity in $H_2{}^{15}O$ study. *Solid lines* are for normal conditions. *Dotted lines* are for misery perfusion conditions. *Dotted dashed lines* are for occlusion conditions

$CMRO_2^m$ tended to become negative values. In detail, for occlusion condition (iii) longer integration time provided smaller error of estimated OEF^m and $CMRO_2^m$. In misery perfusion condition (ii), the error of estimated OEF^m also became smaller error until 300 s, and then the error tended to become negative. The error of estimated $CMRO_2^m$ for condition (ii) is minimized to −1.22% at 180 s accumulation time. In normal condition (i), the error of estimated OEF^m was minimized to −1.9% at 240 s, and the error of estimated $CMRO_2^m$ was minimized to −2.63% at 120 s.

Discussion

In this study, for proper scan protocol of the ARG method in $^{15}O_2$ study, we simulated time dependency of accuracy and variation in physiological parameters with statistical noise and effect of tissue heterogeneity.

S/N ratio in estimated OEF

Variance of pixel counts in reconstructed images is delivered from randomly emitted and detected photon counts and then propagates to estimated OEF and $CMRO_2$ values. Actually, the statistical model of variance of pixel counts does not simply obey the Poisson statistics owing to several data processing (normalization, attenuation, and scatter corrections), which destroy the statistical relationship between expected and observed values. Earlier, there were investigations on developing the statistical model of pixel value [7, 15, 16]. Carson et al. [15] and Watabe et al. [16] modeled statistical variation of pixel value using NEC and then evaluated the adaptability of the model by the phantom and clinical studies. Their approach is simple and accurate enough, and so, we utilized their approach to simulate the noise.

We simulated the TAC $C_t(t)$ from lower to higher count level using three cases of CBF = 20, 50, and 80 (ml/100 g per minute) under three conditions of OEF values (0.2, 0.4, and 0.6), because the variation in OEF depends on the TAC counts level. As shown in Fig. 3, the longer scan time provides better S/N ratio. This figure indicates that the S/N ratio with low OEF and high CBF (Fig. 3c) reaches a plateau earlier than other cases. This is because that later points of TAC with low OEF and high CBF have little impact on the noise of estimates. Because $CMRO_2$ is the product with OEF and CBF, the characteristic of statistical noise of estimated $CMRO_2$ could be propagated from estimated OEF as well as estimated CBF values. Therefore, the maximum S/N ratio of the estimated $CMRO_2$ expects to show the same tendency as the S/N ratio of the estimated OEF if the statistical noise of the CBF was fixed.

In the present study, we assumed the noise-free arterial input function for the simulation. Furthermore, we added noise to arterial input function, but the tendency did not change (data are not shown).

Tissue heterogeneity

We showed that in the mixed region of gray and white matter, the non-linear relationship between physiological parameters and PET counts results in over-/underestimation of the physiological parameters. Figure 5 shows that a lower CBF such as ischemic disease leads to a small error of estimated CBF^m when compared with normal CBF because that effect of the non-linear relationship is less dominant than in the case of a high CBF value. This is consistent with results that Ito et al. [8]

showed high CBF value is more suffered from the tissue heterogeneity when compared with that low CBF value in SPECT study [8]. For the ARG PET study with $H_2{}^{15}O$ study, earlier research by Kanno et al. showed about 13% underestimation in estimated CBF owing to tissue heterogeneity for scan time, 120 s, assuming $CBF^g = 80$, $CBF^w = 20$, $P = 1.0$, and gray matter fraction = 0.5 [9]. Even though there were slight differences in partition coefficient and scan time between Kanno et al. [9] and our study, underestimation in estimated CBF was about 12% for scan time 90 s, assuming $CBF^g = 80$, $CBF^w = 20$, $P = 0.9$, and gray matter fraction = 0.5, which was almost similar results to Kanno et al. [9].

The errors of estimated OEF^m and $CMRO_2{}^m$ are propagated from such error of estimated CBF^m. As shown in Fig. 7, the results of the present study suggest that error of estimated physiological parameters with tissue heterogeneity will variously change positive or negative under the conditions (i), (ii), and (iii) with various scan times. The shorter scan time, the more overestimation was observed for OEF^m under the conditions (i), (ii), and (iii), and $CMRO_2{}^m$ especially under the condition (iii). This may be caused from the underestimation of CBF^m, which can be assumed to be the lower oxygen-15 oxy-hemoglobin supplement than true oxygen-15 oxy-hemoglobin supplement (= observed or simulated PET counts) especially at the early scan time, when the metabolized water component can be neglected. In the longer scan time, the more underestimation was observed for OEF^m under the conditions (i) and (ii) and $CMRO_2{}^m$ especially under the condition (i). There are earlier studies on tissue heterogeneity in estimated OEF for the steady-state method [10, 11]. Without considering error in estimated CBF, Lammertsma and Jones [10] showed that OEF values for every condition were underestimated owing to tissue heterogeneity. Correia et al. [11] investigated the effect of tissue heterogeneity on OEF considering the error in estimated CBF under the condition of the steady state. According to their studies, a small OEF^g value (i.e., $OEF^g = 0.2$, $OEF^w = 0.4$) leads to overestimation in OEF, and a large OEF^g value ($OEF^g = 0.8$, $OEF^w = 0.4$) leads to underestimation in OEF. Interestingly, the overestimation in estimated large OEF^g (i.e., $OEF^g = 0.6$, $OEF^w = 0.45$ especially in occlusion case) in our study was different from the underestimation in estimated large OEF^g by Correia et al. and this may be caused by different methodologies used (steady-state or autoradiography).

To optimize the scan time for the $^{15}O_2$ scan, it is important to consider not only the error in OEF^m and $CMRO_2{}^m$ but also the error in CBF^m derived from the ^{15}O water scan, which is unavoidable factor. Considering the variation of OEF and $CMRO_2$, tissue heterogeneity, and applicability for clinical study, the optimal scan time of 3 min is suggested owing to following three reasons:

1. At the point of S/N of OEF and $CMRO_2$, the longer scan time is adequate (Fig. 3).
2. In terms of estimating OEF under circumstance of tissue heterogeneity, the longer scan time is adequate (Fig. 7a).
3. As shown in Fig. 7b, longer scan time has been required for $CMRO_2{}^m$ under the condition (iii). Conversely, shorter scan time has been required for $CMRO_2{}^m$ under the condition (i). The minimum error of $CMRO_2{}^m$ under the condition (ii) was achieved at the 180 s scan time.

Alpert et al. [18] earlier commented that factors of optimal scan time for oxygen-15-labeled water study are grouped as (1) the total observation time period, (2) scan and blood sampling protocol, and (3) the type and magnitude of tracer administration. This grouping can also be applied to oxygen-15 gas study, but most facilities have already installed the equipments, and it is not so easy to change the blood sampling protocol and supplement of tracer. In this study, we discussed the optimal scan time under the conditions of fixed administration dose, inhalation time, and blood sampling protocols. It must be noted that if administration protocol is changed from 1-min inhalation without breath control to others, present optimization of scan time may not be suited.

Recently, a rapid protocol with a single-PET scan with dual-tracer ($^{15}O_2$ and $H_2{}^{15}O$) administration method was developed [19, 20]. They employed integrated PET data for 90 s in H_2O phase and 180 s in O_2 phase. Our strategies to optimize the scan duration could be applied for this rapid protocol to estimate CBF, OEF, and $CMRO_2$ accurately.

Kobayashi et al. [21] examined relationship between count-based OEF and scan duration. They used quantitative OEF as a standard to evaluate optimal scan duration. Although their approach to obtain OEF is different from ours, as shown in this article, the tissue heterogeneity could be another important attribution for determining the optimal scan duration.

Conclusions

In this study, we performed computer simulation studies of $^{15}O_2$ gas inhalation protocol with the ARG method. Tissue heterogeneity largely affects the quantification of estimated OEF and $CMRO_2$, and is a dominant factor in the optimization of scan time in oxygen-15 gas study. According to these simulated results, the optimal scan time for $^{15}O_2$ gas inhalation protocol is suggested to be 3 min for ischemic disease.

Acknowledgments This study was supported in part by the Grant-in-Aid for Young Scientists (B) from the Ministry of Education, Culture, Sports, Science and Technology (19700395), Japan.

References

1. Ter-Pogossian MM, Herscovitch P. Radioactive oxygen-15 in the study of cerebral blood flow, blood volume, and oxygen metabolism. Semin Nucl Med 1985;15:377–94.
2. Baron JC, Bousser MG, Rey A, Guillard A, Comar D, Castaigne P. Reversal of focal "misery-perfusion syndrome" by extra-intracranial arterial bypass in hemodynamic cerebral ischemia: a case study with 15O positron emission tomography. Stroke 1981;12:454–9.
3. Gibbs JM, Wise RJ, Leenders KL, Jones T. Evaluation of cerebral perfusion reserve in patients with carotid-artery occlusion. Lancet 1984;11:310–4.
4. Mintun MA, Raichle ME, Martin WR, Herscovitch P. Brain oxygen utilization measured with O-15 radiotracers and positron emission tomography. J Nucl Med 1984;25:177–87.
5. Jones SC, Greenberg JH, Reivich M. Error analysis for the determination of cerebral blood flow with the continuous inhalation of 15O-labeled carbon dioxide and positoron emission tomograph. J Comput Assist Tomogr 1982;6:116–24.
6. Hatazawa J, Fujita H, Kanno I, Satoh T, Iida H, Miura S. Regional cerebral blood flow, blood volume, oxygen extraction fraction and oxygen utilization rate in normal volunteers measured by the autoradiographic and the single inhalation method. Ann Nucl Med 1995;9:15–21.
7. Kanno I, Iida H, Miura S, Murakami M. Optimal scan time of oxygen-15-labeled water injection method for measurement of cerebral blood flow. J Nucl Med 1991;32:1931–4.
8. Ito H, Shidahara M, Inoue K, Goto R, Kinomura S, Taki Y, et al. Effects of tissue heterogeneity on cerebral vascular response to acetazolamide stress measured by an I-123-IMP autoradiographic method with single-photon emission computed tomography. Ann Nucl Med 2005;19:251–60.
9. Kanno I, Iida H, Miura S, Murakami M, Takahashi K, Sasaki H, et al. A system for cerebral blood flow measurement using an $H_2{}^{15}O$ autoradiographic method and positron emission tomography. J Cereb Blood Flow Metab 1987;7:143–53.
10. Lammertsma AA, Jones T. Low oxygen extraction fraction in tumours measured with the oxygen-15 steady state technique: effect of tissue heterogeneity. Br J Radiol 1992;65:697–700.
11. Correia JA, Aplert NM, Buxton RB, Ackerman RH. Analysis of some errors in the measurement of oxygen extraction and oxygen consumption by the equilibrium inhalation method. J Cereb Blood Flow Metab 1985;5:591–9.
12. Iida H, Kanno I, Miura S, Murakami M, Takahashi K, Uemura K. A determination of the regional brain/blood partition coefficient of water using dynamic positron emission tomography. J Cereb Blood Flow Metab 1989;9:874–85.
13. Shidahara M, Watabe H, Kim KM, Oka H, Sago M, Hayashi T, et al. Evaluation of a commercial PET tomograph-based system for the quantitative assessment of rCBF, rOEF and $rCMRO_2$ by using sequential administration of ^{15}O-labeled compounds. Ann Nucl Med 2002;16:217–28.
14. Iida H, Jones T, Miura S. Modeling approach to eliminate the need to separate arterial plasma in oxygen-15 inhalation positron emission tomography. J Nucl Med 1993;34:1333–40.
15. Carson RE, Yan Y, Daube-Witherspoon ME, Freedman N, Bacharach SL, Herscovitch P. An approximation formula for the variance of PET region of interest values. IEEE Med Imaging 1993;12:240–50.
16. Watabe H, Endres CJ, Breier A, Schmall B, Eckelman WC, Carson RE. Measurement of dopamine release with continuous infusion of [11C]raclopride: optimization and signal-to-noise considerations. J Nucl Med 2000;41:522–30.
17. Strother SC, Casey ME, Hoffman EJ. Measuring PET scanner sensitivity: relating count rates to image signal-to-noise ratios using noise equivalent counts. IEEE Trans Nucl Sci 1990;37:783–8.
18. Alpert N. Optimization of regional cerebral blood flow measurements with PET (comment on J Nucl Med 1991;32:1931–4). J Nucl Med 1991;32:1934–6.
19. Kudomi N, Hayashi T, Teramoto N, Watabe H, Kawachi N, Ohta Y, et al. Rapid quantitative measurement of $CMRO_2$ and CBF by dual administration of ^{15}O-labeled oxygen and water during a single PET scan-a validation study and error analysis in anesthetized monkeys. J Cereb Blood Flow Metab 2005;25:1209–24.
20. Kudomi N, Watabe H, Hayashi T, Iida H. Separation of input function for rapid measurement of quantitative $CMRO_2$ and CBF in a single PET scan with a dual tracer. Phys Med Biol 2007;52:1893–908.
21. Kobayashi M, Kudo T, Tsujikawa T, Isozaki M, Arai Y, Fujibayashi Y, et al. Shorter examination method for the diagnosis of misery perfusion with count-based oxygen extraction fraction elevation in ^{15}O-Gas PET. J Nucl Med 2008;49:242–6.

映像情報
Medical
A monthly Journal of Medical Imaging and Information

別刷

産業開発機構株式会社

高解像度定量ピンホールSPECTイメージング －小動物から臨床へ－

奈良先端科学技術大学院大学 情報科学研究科[*1]／国立循環器病センター研究所 先進医工学センター 放射線医学部[*2]／筑波大学大学院 システム情報工学研究科[*3]

銭谷 勉[*1,2]／渡部浩司[*2]／工藤博幸[*3]／飯田秀博[*2]

はじめに

創薬や新規治療法の評価を目的とした前臨床研究において、ラットやマウスなどの小動物モデルを利用した*in vivo*イメージングは必要不可欠である。さらに近年の分子イメージング分野の発展に伴い、小動物専用イメージング装置がさかんに開発、製品化されている。その中でもPET（Positron Emission Tomography）やSPECT（Single Photon Emission Computed Tomography）といった放射性同位元素を用いる核医学的検査手法は高い感度を有し、トレーサの集積に対して正確に比例した信号強度を提示するため、病態生理や病態生化学的な変化を定量的に評価することができることから、重要な役割を担っている。

臨床用SPECT装置の解像度は10mm程度であり、小動物の撮像には不十分である。ピンホールコリメータを利用すると小視野領域の像が拡大され、1mm以下の高解像度で小動物のイメージングが可能となる[1]。このため、現在実用化されている小動物用SPECT装置は、ほとんどピンホールコリメータを採用している[2]。ピンホールコリメータで撮像した場合、体軸方向の画像歪とデータ欠損（トランケーション）という2つの定量性を劣化させる問題がある。われわれはこれらの問題に対して、2軸収集法およびトランケーションを許す撮像・画像再構成法を開発した。

本稿では、ピンホールSPECTによる高解像度イメージング技術を簡単に述べた上で、ピンホールSPECTにおいて定量画像を得るためにわれわれが開発した、画像歪とトランケーションの問題を改善するための撮像・画像再構成技術を概説する。また、これらの技術を応用した小動物SPECT装置についても述べたいと思う。

最近われわれは、ピンホールSPECTのヒトのような大きな被写体を対象とする局所高解像度定量イメージングへの利用を考えている。このためのトランケーションを許す画像再構成法に関しても、最後に述べる。

ピンホールコリメータによる高解像度SPECT

SPECT装置は、原理的に放射性同位元素から放出されるガンマ線の飛来方向を特定するためのコリメータを必要とする。臨床用のSPECT装置では、一般的にパラレルホールコリメータが用いられており、解像度は10mm程度である。小動物イメージングでは対象臓器も小さいため、それに伴って高解像度が要求される。ピンホールコリメータは撮像対象がコリメータに近いほど像をより拡大できるため、空間解像度および感度を高くできる（**図1**）。1mm以下の解像度も比較的容易に実現できるため、小動物のイメージングに適している。

ピンホールSPECTにおける画像歪の改善

ピンホールコリメータを用いたSPECT装置では、原理上3次元のデータ収集を行っているが、コーンビーム型CTの3次元画像再構成法が必要となる。従来のピンホールSPECTでは、単一の円軌道で投影データを収集し、解析的なFiltered Back-Projection（FBP）法によって画像再構成していた。この画像再構成法によると、**図2（上）**のように再構成された画像は体軸方向に歪み、視野内の解像度が不均一となるため定量評価が困難であり、研究の域を脱しなかった。FBP法に代えてOSEM（Ordered Subsets Expectation Maximization）などの統計学に基づいた逐次近似画像再構成法を適用することで、画像の中央付近では歪みが大幅に改善された[3]。しかし、視野の周辺では依然として解像度の劣化は残っている。

われわれは、この原因を投影データの不完全性に起因するものと仮説を立て、Tuyが導出したコーンビームCTで、3次元画像再構成に必要な完全データを収集するための条件「被写体と交わるすべての平面が焦点（ピンホール）軌道と交わる」[4]を満たすように撮像軌道を**図2（下）**のような複数回転軸軌道とし、